Journal of Fluids and Structures 18 (2003) 441–454

JOURNAL OF FLUIDS AND STRUCTURES

www.elsevier.nl/locate/jnlabr/yjfls

On uniform planar shear flow around a circular cylinder at subcritical Reynolds number

D. Sumner*, O.O. Akosile

Department of Mechanical Engineering, University of Saskatchewan, 57 Campus Drive, Saskatoon, Saskatchewan, Canada S7N 5A9

Received 10 July 2002; accepted 3 August 2003

Abstract

An experimental investigation was conducted of a circular cylinder immersed in a uniform planar shear flow, where the approach velocity varies across the diameter of the cylinder. The study was motivated by some apparent discrepancies between numerical and experimental studies of the flow, and the general lack of experimental data, particularly in the subcritical Reynolds number regime. Of interest was the effect of shear on the vortex-shedding frequency and the mean aerodynamic forces, including the direction and origin of the steady mean lift force experienced by the cylinder, which has been the subject of contradictory results in the literature and for which measurements have rarely been reported. The circular cylinder was tested at Reynolds numbers from $\mathrm{Re} = 4.0 \times 10^4$ to 9.0×10^4, and the dimensionless shear parameter ranged from $K = 0.02$ to 0.07, which corresponds to a flow with low to moderate shear. The results from both the present and previous studies show that low to moderate shear causes a small increase in the Strouhal number, an increase in the mean base pressure coefficient, a reduction in the mean drag force coefficient, and a small mean lift force directed towards the low-velocity side. These effects are consistent with a narrowing, or reduction in width, of the cylinder near wake, which is supported by an asymmetric mean static pressure distribution on the surface of the cylinder.

1. Introduction

A circular cylinder immersed in a uniform approach flow has been a well-studied problem in fluid mechanics. The cylinder experiences a high mean drag force coefficient and, for a wide range of Reynolds number, the flow is marked by the alternate, periodic shedding of Kármán vortices. The tendency towards vortex-induced vibration of the circular cylinder has been an important motivating factor for its study. In many practical applications, a cylindrical structure is immersed in a nonuniform approach flow, which may influence the vortex-shedding behaviour and the aerodynamic forces acting upon it. Examples include a circular cylinder immersed in a mixing layer (Kiya et al., 1979), a circular cylinder situated in the wake of another cylinder (Zdravkovich, 1977), or a circular cylinder adjacent to a plane wall boundary (Bearman and Zdravkovich, 1978). The simplest case of a nonuniform approach flow is a uniform shear flow, where there is a linear variation of the approach flow velocity, yielding a constant velocity gradient and vorticity. The study of a uniform shear flow is a common starting point for investigations of bluff bodies in more complex nonuniform approach flows.

There are two basic configurations for a circular cylinder in a shear flow: in axial shear flow, the approach velocity, $U(z)$, varies linearly along the span of the cylinder, L (see Fig. 1(a)); in planar shear flow, the approach velocity, $U(y)$, varies across the diameter of the cylinder, D (see Fig. 1(b)). The axial flow configuration (Fig. 1(a)) is applicable to the

*Corresponding author. Tel.: +1-306-966-5537; fax: +1-306-966-5427.
E-mail address: david.sumner@usask.ca (D. Sumner).

0889-9746/$ - see front matter © 2003 Elsevier Ltd. All rights reserved.
doi:10.1016/j.jfluidstructs.2003.08.004

Nomenclature

A	velocity gradient (s^{-1})
AR	cylinder aspect ratio
C_D	mean drag force coefficient
C_L	mean lift force coefficient
C_P	mean static pressure coefficient
C_T	mean total aerodynamic force coefficient
D	cylinder diameter (m)
F_D	mean drag force (N)
F_L	mean lift force (N)
f	vortex shedding frequency (Hz)
K	shear parameter
L	cylinder span (m)
P	static pressure (Pa)
P_C	centre-line freestream static pressure (Pa)
Re	reynolds number
St	strouhal number
U	approach velocity (m/s)
U_C	centre-line velocity (m/s)
x	streamwise direction (m)
y	cross-stream direction (m)
β	direction of the mean total aerodynamic force (deg)
θ	angular position on the surface of the cylinder (deg)
v	kinematic viscosity (m^2/s)
ρ	density (kg/m^3)

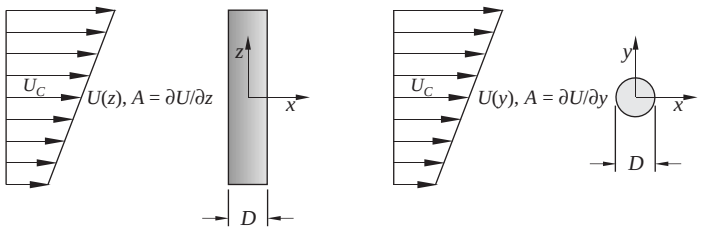

Fig. 1. Circular cylinder in a uniform shear flow: (a) axial shear and (b) planar shear.

study of submarine cables and offshore platforms immersed in ocean currents, and to simplified buildings in the atmospheric boundary layer, for example. These applications and others have motivated a number of experimental and numerical studies of bluff bodies in an axial shear flow, for both stationary and oscillating cylinders, which have been reviewed by Griffin (1985). Important effects of axial shear flow on the circular cylinder include cellular vortex-shedding, spanwise variation of the base pressure and the sectional drag force coefficient, and a lower critical Reynolds number.

Less well studied is a circular cylinder immersed in a planar shear flow (Fig. 1(b)). This problem is applicable to undersea pipelines immersed in an ocean current or near the seabed, or to long-span bridges immersed in the atmospheric boundary layer, for example. The uniform planar shear flow velocity profile, $U(y)$, is given by

$$U(y) = U_C + Ay \tag{1}$$

for constant velocity gradient, A ($= \mathrm{d}U/\mathrm{d}y$), cross-stream coordinate, y, and the centre-line value of the approach velocity, U_C (Fig. 2). For a circular cylinder of diameter, D, the Reynolds number is based on the centre-line velocity, i.e., $Re = U_C D/v$, where v is the kinematic viscosity of the fluid. The velocity gradient of the uniform shear flow is characterized by a dimensionless shear parameter, $K = AD/U_C$. The shear parameter identifies a flow as having no

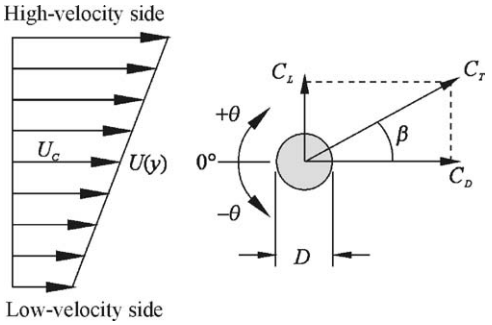

Fig. 2. Nomenclature for a circular cylinder in a uniform planar shear flow.

shear ($K = 0$), low to moderate shear (K being small), or strong shear (K being large), although there is no commonly accepted definition of what constitutes low, moderate, or strong shear.

2. Background

Uniform planar shear flow around a circular cylinder has been studied theoretically and numerically to a much greater extent than experimentally. Zdravkovich (1997) has reviewed several of the theoretical models for a circular cylinder in a planar shear flow. Numerical studies by Jordan and Fromm (1972), Tamura et al. (1980), Yoshino and Hayashi (1984), Lei et al. (2000), and Wu and Chen (2000), have been conducted mostly at low Reynolds numbers, where the flow around a circular cylinder in uniform flow remains two-dimensional. Also, there have been several numerical studies of the *square* cylinder in a uniform planar shear flow, also at low Reynolds numbers, by Ayukawa et al. (1993), Hwang and Sue (1997), and Saha et al. (1999, 2001). However, because the square cylinder has fixed separation points, its behaviour in a planar shear flow is different than the circular cylinder, where the separation points are free to move.

There have been relatively few experimental investigations of a circular cylinder in a uniform planar shear flow (see Fig. 2), particularly so at high subcritical Reynolds numbers, i.e., $10^4 < \mathrm{Re} < 10^5$. Previous experimental studies of the circular cylinder by Adachi and Kato (1975), Kiya et al. (1980), Hayashi et al. (1991, 1993), Kwon et al. (1992), and Sung et al. (1995), and the range of K which has been investigated, are summarized in Table 1. Most of these studies have been conducted in the low subcritical regime, i.e., $\mathrm{Re} < 10^4$, and in flows with what may be considered low to moderate shear, $K = 0.01-0.15$. The experiments of Hayashi et al. (1991, 1993), at $\mathrm{Re} = 6.0 \times 10^4$, provide some of the only published experimental data in the high subcritical regime. This lack of experimental data has led to a number of unresolved issues pertaining to the influence of shear on the vortex-shedding frequency and the aerodynamic forces.

The vortex-shedding frequency, f, is represented in dimensionless form by the Strouhal number, St ($= fD/U_C$). Experimental studies by Kiya et al. (1980) and Kwon et al. (1992), both conducted in the low subcritical regime, have shown that the Strouhal number increases with K in flows with low to moderate shear; there have been no reported measurements of the Strouhal number in the upper subcritical regime. The numerical study by Lei et al. (2000), for $\mathrm{Re} = 80-1000$, has reported the opposite trend, that the Strouhal number decreases with K, although the effect was small. The numerical studies for the square cylinder in a uniform planar shear flow (Ayukawa et al., 1993; Hwang and Sue, 1997; Saha et al., 1999, 2001) also report a small decrease in Strouhal number with K. Some additional measurements of the Strouhal number are therefore needed to clarify its behaviour.

For the mean drag force coefficient, C_D ($= 2F_D/\rho U_C^2 DL$, where F_D is the mean drag force, ρ is the fluid density), there is general agreement among the experimental studies (Adachi and Kato, 1975; Hayashi et al., 1991, 1993; Kwon et al., 1992) and the numerical studies for circular and square cylinders (Ayukawa et al., 1993; Hwang and Sue, 1997; Lei et al., 2000). These studies have shown that the mean drag coefficient decreases with K throughout the subcritical regime. An exception is the numerical study by Tamura et al. (1980), which showed the drag coefficient increases with K at low Reynolds numbers, $\mathrm{Re} = 40-80$.

For the mean lift force coefficient, C_L ($= 2F_L/\rho U_C^2 DL$, where F_L is the mean lift force), there is still some disagreement over its magnitude, direction, and origin, mainly because there have been very few reported measurements. The experiments of Adachi and Kato (1975) and Hayashi et al. (1991, 1993) have shown the lift coefficient to be negative, i.e., directed towards the low-velocity side (see Fig. 2), and the magnitude of the lift coefficient to increase (i.e., become more negative) with K. Their conclusions were based on measurements of the static pressure

Table 1
Experimental studies of a circular cylinder in a uniform planar shear flow

Researchers	Method	Reynolds number, Re	Shear parameter, K	Velocity nonuniformity	Turbulence intensity	Aspect ratio, AR	Solid blockage ratio
Adachi and Kato (1975)	Wind tunnel Honeycomb	2670–10,700	0.011–0.04				
Hayashi et al. (1991)	Wind tunnel Honeycomb	6.0×104	0.15				
Hayashi et al. (1993)	Wind tunnel Unequally spaced rods/honeycomb	6.0×104	0.03–0.15	2%	1.0–2.3%	5	6.7%
Kiya et al. (1980)	Liquid channel Honeycomb	35–1500	0.05–0.25	3%		2–12.5	2.7–17%
Kwon et al. (1992)	Water tunnel Channels with variable flow rate	600–1600	0.05–0.25	1.5%	$<1.5\%$	5.2–13	6.7–16%
Sung et al. (1995)	Water tunnel Channels with variable flow rate	600–1200	0.05–0.15	1.5%	$<1.5\%$	8.7	10%
Current study	Wind tunnel	4.0×104–9.0×104	0.02–0.07	3%	$<1.5\%$	12.3–18.4	1.8–2.7%

distribution on the surface of the cylinder, expressed as a dimensionless pressure coefficient, $C_P(\theta)$ ($= 2(P(\theta)\text{-}P_C)/\rho U_C^2$, where $P(\theta)$ is the local static pressure distribution at angle θ (see Fig. 2), and P_C is the centre-line freestream static pressure), which showed movement of the stagnation, minimum pressure, and separation points on the surface of the cylinder in a shear flow. Numerical studies of the circular cylinder in shear flow by Jordan and Fromm (1972) and Lei et al. (2000) agree with these experimental results, with C_L being negative, i.e., directed towards the low-velocity side. Other numerical studies, by Tamura et al. (1980) and Yoshino and Hayashi (1984), have shown the opposite result, that the lift coefficient is positive, i.e., directed towards the high-velocity side (see Fig. 2). A positive lift coefficient has also been observed for the square cylinder in a uniform shear flow (Ayukawa et al., 1993; Hwang and Sue, 1997), but this difference may be attributed to its sharp corners, which fix the locations of the square cylinder's separation points. Furthermore, the numerical study by Wu and Chen (2000) concluded that the direction of C_L may be either positive or negative depending on the degree of shear. Some further experiments are therefore needed to establish the direction and magnitude of the lift coefficient.

The disagreement among the numerical and experimental studies, and the scarcity of sufficient experimental data, particularly at high subcritical Reynolds numbers, have motivated the present experimental investigation of a circular cylinder in a uniform planar shear flow. The study was undertaken for $\mathrm{Re} = 4.0 \times 10^4 - 9.0 \times 10^4$ and at low to moderate shear, $K = 0.02 - 0.07$.

3. Experimental details

Experiments were conducted in a low-speed, closed-return wind tunnel, with a test-section of 0.91 m (height) $\times$ 1.13 m (width) $\times$ 1.96 m (length). The test-section floor was fitted with a ground plane. Under uniform flow conditions, the longitudinal freestream turbulence intensity is 0.6% and the velocity nonuniformity in the central portion of the test-section, outside the test-section wall boundary layers, is 0.5%.

Two smooth circular cylinders, $D = 0.032$ and 0.048 m, were tested, separately, in both a uniform flow and a sheared flow. Each cylinder was mounted vertically from a six-component force balance located outside and beneath the wind tunnel test-section in order to directly measure F_D and F_L (see Fig. 3(a)). The cylinders were mounted between a pair of rectangular end plates designed according to the recommendations of Szepessy (1993). The end plates were isolated from both the cylinder and the force balance (see Fig. 3(b)). The 0.032 and 0.048 m cylinders had aspect ratios of $\mathrm{AR} = L/D = 18.4$ and 12.3, and solid blockage ratios of 1.8% and 2.7%, respectively. No wall interference corrections were made. Previous studies have been conducted at much lower aspect ratios and higher blockage ratios, where specified (see Table 1) and without end plates. Each cylinder was instrumented with static pressure taps (of 0.8 mm diameter), and was rotated with the force balance in small angular increments to measure the $C_P(\theta)$ distribution at mid-span (see Fig. 3). The Reynolds number range of the experiments was $\mathrm{Re} = 4 \times 10^4 - 9 \times 10^4$.

Reference flow conditions and velocity profiles were measured with a Pitot-static probe (United Sensor, 3.2 mm diameter) and Datametrics Barocell absolute and differential pressure transducers. Static pressure measurements on the surface of the cylinder were made with another Datametrics differential pressure transducer. Vortex-shedding frequencies were measured with a single-sensor hot-wire probe (TSI Model 1210-T1.5) and a TSI IFA-100 constant temperature anemometer. The probe was positioned at mid-span in the cylinder wake, at $x/D = 3.0$ and $y/D = 1.0$ measured from the centre of the cylinder, using a three-axis computer-controlled traversing system. Data were acquired with a Pentium II microcomputer, a National Instruments AT-MIO-64F-5 12-bit multifunction board and LabVIEW software.

The measurement uncertainty was estimated at ± 0.03 N for the aerodynamic forces and ± 0.02 for the $C_P(\theta)$ data. The uncertainty in the angular position of the cylinder was estimated at $\pm 0.5^\circ$. Representative error bars for these and other measurements are included in the figures.

4. Shear flow generator

A number of methods have been adopted to produce a shear flow in a wind tunnel. Ideally, the method must produce a smooth velocity profile with a low turbulence level. Designs for shear flow generators have used a variety of techniques: an array of differentially spaced circular rods (Owen and Zienkiewicz, 1957), contoured honeycombs (Kotansky, 1966; Ahmed and Lee, 1997), curved screens (Castro, 1976), separate channels with adjustable blockage (Karnik and Tavoularis, 1987), or differentially spaced flat places (Phillips et al., 1999).

In the present study, a contoured honeycomb shear flow generator was installed at the entrance to the test-section, immediately downstream of the contraction exit (see Fig. 3(a)). The shape of the honeycomb was designed using the

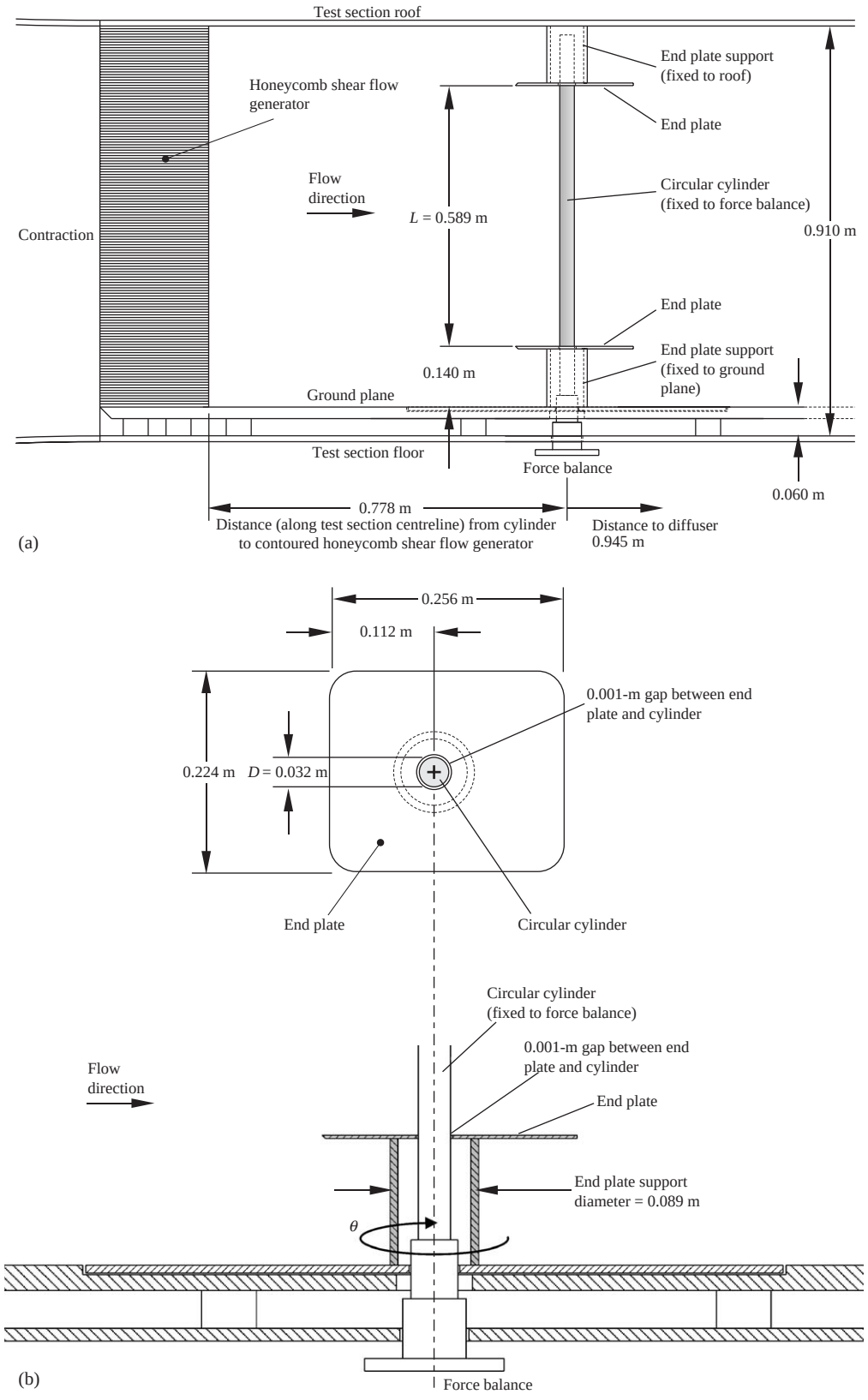

Fig. 3. (a) Experiment set-up in the wind tunnel, $D = 0.032$ m and (b) detail of end plates and end plate supports.

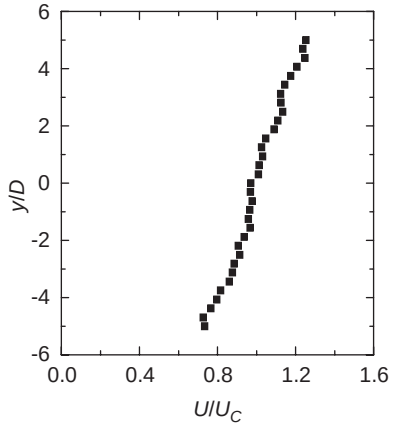

Fig. 4. Uniform shear velocity profile 0.6 m downstream of the shear flow generator, at the test-section centre-line, $U_C = 24.3\,\mathrm{m/s}$, $A = 36.7\,\mathrm{s}^{-1}$, $K = 0.05$ (for 0.032 m cylinder), nonuniformity of 2.4%.

method of Kotansky (1966) to achieve the desired velocity gradient. Sheets of "core plast" of varying length were stacked vertically to comprise the shear flow generator. The velocity gradient ranged from $A = 4.9-36.4\,\mathrm{s}^{-1}$ depending on the velocity upstream of the honeycomb and the contour shape employed. The length of the wind tunnel section and other operational constraints imposed a limit on the maximum value of the velocity gradient that could be attained (Akosile and Sumner, 2001; Akosile, 2002). Some fine tuning of the honeycomb shape was necessary to ensure a smooth velocity profile, which was typically uniform to within 3% across the test-section. The longitudinal freestream turbulence intensity was less than 1.5% downstream of honeycomb. A representative velocity profile is shown in Fig. 4. Further design details are given by Akosile and Sumner (2001) and Akosile (2002).

One of the challenges of using a shear flow generator is the interdependence of the shear parameter and the Reynolds number, i.e., one variable cannot be changed independently of the other. For the honeycomb shear flow generator used in the present study, K was mostly a weak function of Re. When cylinders of different diameters are used to extend the range of shear parameters and Reynolds numbers that can be tested, then the cylinder aspect ratio and the solid blockage ratio cannot be held constant as K and Re are varied. For instance, Kwon et al. (1992) used several cylinders to achieve their large range of K and Re (see Table 1). By doing so, the possibility that changes in the aspect ratio and the solid blockage ratio had an impact on the effects of shear observed by Kwon et al. (1992) cannot be completely ignored.

5. Results and discussion

Each circular cylinder was tested first under no-shear flow conditions, $K = 0$, with the shear flow generator removed. This was followed by the experiments in a uniform planar shear flow, with the shear flow generator installed, which yielded $K = 0.02-0.07$ at $\mathrm{Re} = 4.0 \times 10^4 - 9.0 \times 10^4$.

5.1. Strouhal number

The Strouhal number data, Fig. 5, showed that low to moderate shear, $K = 0.02-0.07$, had no significant influence on vortex shedding from the circular cylinder at subcritical Reynolds numbers. A small reduction in the Strouhal number may be observed in Fig. 5, but the reduction falls within the uncertainty limits of the experiments. These experimental results are consistent with the numerical studies of Ayukawa et al. (1993), Hwang and Sue (1997), Lei et al. (2000), and Saha et al. (2001), which showed a very small reduction in Strouhal number with K. To the knowledge of the authors, these Strouhal data are some of the first reported for a circular cylinder in a uniform planar shear flow in the subcritical Reynolds number regime.

The present results appear, at first, to contradict the experimental results of Kiya et al. (1980) and Kwon et al. (1992), which have shown the Strouhal number to increase with K. A possible explanation for the different trends is that the effects of low aspect ratio and high blockage may have unduly influenced the results from these two previous studies (see Table 1); the solid blockage ratio for Kwon et al. (1992) was particularly high, and ranged from 6.7% to 16%. Also,

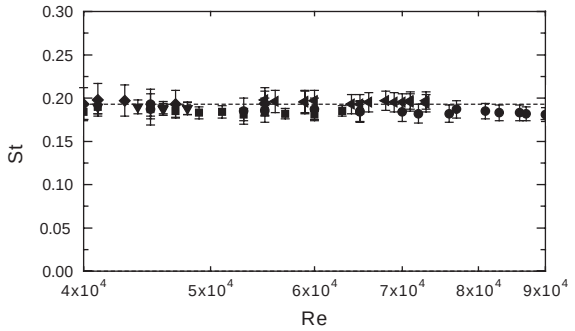

Fig. 5. Strouhal number data for a circular cylinder in a uniform planar shear flow: ■, $K = 0.02$; ●, $K = 0.03$; ▲, $K = 0.04$; ▼, $K = 0.05$; ♦, $K = 0.06$; ◀, $K = 0.07$; -----, no shear case, $K = 0$.

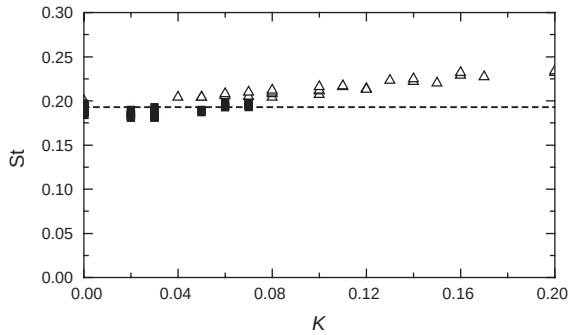

Fig. 6. Strouhal number data for a circular cylinder in a uniform planar shear flow: ■, present study, $Re = 4.0 \times 10^4 - 9.0 \times 10^4$, AR = 12.7−18.4; △, Kwon et al. (1992), Re = 600−1500, AR = 5.2−13; ----, no shear case, $K = 0$.

there is a high degree of scatter in the Strouhal data of Kiya et al. (1980). Furthermore, the experiments of Kiya et al. (1980) and Kwon et al. (1992) were conducted at much lower Reynolds numbers, than the present study, Re = 35−1600, where the near-wake structure and vortex-shedding mechanism exhibit some differences from the subcritical regime.

However, the experiments of Kiya et al. (1980) and Kwon et al. (1992) were also conducted at higher shear parameters, $K = 0.05-0.15$, than the present study (see Table 1). When the present data and some of the published experimental data are plotted together (see Fig. 6), there is a consistent behaviour of the Strouhal number increasing with K, indicating that higher levels of shear have a more pronounced effect on Kármán vortex shedding. This increase in the vortex-shedding frequency may be caused by a narrowing of the near-wake region behind the circular cylinder in a planar shear flow, compared to the no-shear case. Such a relationship between the size of the near-wake region and the shedding frequency has been found in studies of two side-by-side circular cylinders, for example, when the gap flow is deflected (or biased) towards one of the two cylinders (Sumner et al., 1999). The biased gap flow creates a narrow near-wake region behind one of the cylinders, which has a higher vortex-shedding frequency than a single cylinder, and a wide near-wake region behind the other cylinder, which has a lower vortex-shedding frequency than a single cylinder. Nevertheless, because of the Reynolds number difference between the studies, it still remains possible that the effect of shear on the shedding frequency may be more pronounced, or even different, at lower Reynolds numbers.

5.2. Aerodynamic forces

The circular cylinder was found to experience both a mean drag force and a mean lift force in the planar shear flow; see Figs. 7 and 8. The mean aerodynamic forces were obtained by two methods: (i) direct measurement using the wind tunnel force balance, for $Re = 4.0 \times 10^4 - 9.0 \times 10^4$ (see Figs. 7 and 8); and (ii) integrating the surface static pressure distribution, at $Re = 7.0 \times 10^4$ (see Table 2). The force data obtained from the pressure measurements are discussed in Section 5.3.

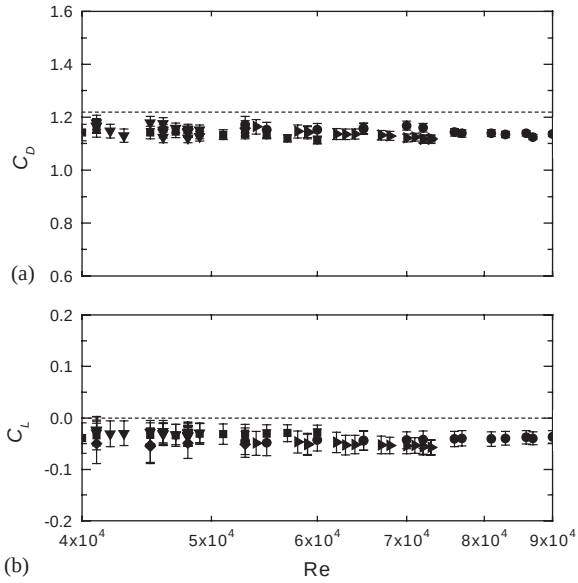

Fig. 7. Mean aerodynamic forces for a circular cylinder in a uniform planar shear flow: (a) mean drag coefficient and (b) mean lift coefficient. Symbols as in Fig. 5.

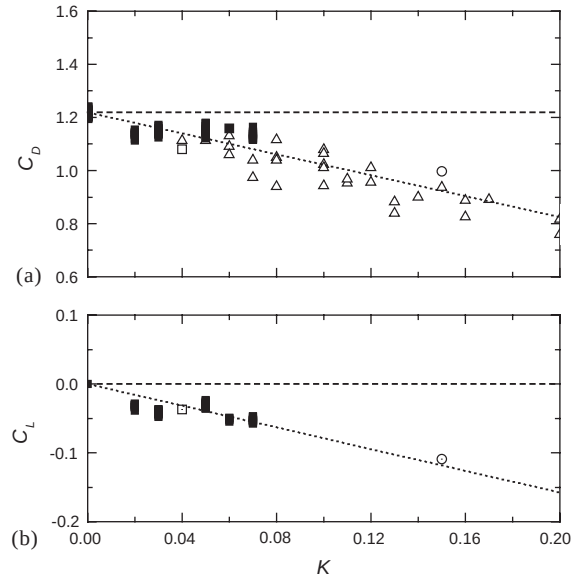

Fig. 8. Mean aerodynamic forces for a circular cylinder in a uniform planar shear flow: (a) mean drag coefficient and (b) mean lift coefficient: ■, present study, $Re = 4.0 \times 10^4 - 9.0 \times 10^4$, AR = 12.7−18.4; □, Adachi and Kato (1975), $Re = 8 \times 10^3$; ○, Hayashi et al. (1991), $Re = 6.0 \times 10^4$, AR = 5; △, Kwon et al. (1992), Re = 600 to 1500, AR = 5.2−13; - - - - -, no shear case, $K = 0$. Trend lines (dotted) shown for illustration purposes only.

The force balance measurements of the mean drag coefficient, C_D, Fig. 7(a), showed that low to moderate shear lowers the mean drag coefficient of the circular cylinder compared to the no-shear case, $K = 0$. This is consistent with all of the existing experimental results (Adachi and Kato, 1975; Hayashi et al., 1991, 1993; Kwon et al., 1992) and several of the numerical studies (Ayukawa et al., 1993; Hwang and Sue, 1997; Lei et al., 2000) for both circular and square cylinders. When the present data and some of the published data are plotted together (see Fig. 8(a)), higher levels

Table 2
Aerodynamic force data for a circular cylinder in a uniform planar shear flow, including data from Adachi and Kato (1975) and Hayashi et al. (1991)

	Re	C_D		C_L		$\lvert C_L/C_D \rvert$		C_T		β		Stagnation point location
		Force balance	Pressure	Force balance	Pressure	Force balance	Pressure	Force balance	Pressure	Force balance	Pressure	
$K = 0$	7.4×10^4	1.222	1.313	–0.003	–0.006	0.002	0.005	1.222	1.313	0°	0°	$\theta = 0°$
$K = 0.04$ (Adachi and Kato, 1975)	0.8×10^4		1.080		–0.037		0.034		1.081		–2°	
$K = 0.07$	7.0×10^4	1.121	1.195	–0.055	–0.034	0.049	0.028	1.195	1.190	–3°	–5°	$\theta = +1°$
$K = 0.15$ (Hayashi et al., 1991)	6.0×10^4		0.997		–0.109		0.109		1.003		–6°	$\theta = +6°$

Measurement uncertainty in C_D and C_L: ± 0.015 from force balance, ± 0.025 from the pressure distribution.

of shear are seen to have a more pronounced effect on the lowering of the mean drag coefficient. This tendency is consistent throughout the subcritical regime, i.e., it is independent of Reynolds number. The lowering of the cylinder drag coefficient may be caused by a narrowing of the near-wake region, or the near-wake width (Griffin, 1981), which was suggested in Section 5.1 as a possible explanation for the increase in the Strouhal number with K.

The force balance measurements of the mean lift coefficient, C_L (see Fig. 7(b)), show that the circular cylinder in a uniform planar shear flow experiences a small mean lift force. The negative sign indicates that this force is directed towards the side of the cylinder experiencing the lower velocity (Fig. 2). This result is consistent with the limited experimental data of Adachi and Kato (1975) and Hayashi et al. (1991, 1993), amounting to only two data-points (see Fig. 8(b)), as well as the numerical results of Jordan and Fromm (1972) and Lei et al. (2000). The results in Fig. 8(b) show that the magnitude of the mean lift coefficient increases with K, i.e., the lift coefficient becomes more negative as K increases. As will be shown in Section 5.3, the mean lift coefficient is caused by an asymmetric mean pressure distribution on the surface of the cylinder.

The cylinder's mean lift coefficient is very small compared to the drag coefficient, with a lift-to-drag ratio of only $|C_L/C_D| = 0.049$ at $K = 0.07$ (see Table 2). Consequently, there is a large measurement uncertainty associated with the mean lift coefficient. This uncertainty is indicated by the error bars in Fig. 7(b); Adachi and Kato (1975) and Hayashi et al. (1991, 1993) did not provide estimates of their measurement uncertainty. In the present study, the most significant contributor to the uncertainty was the angular positioning error of the cylinder and the force balance to which it was attached, which was estimated at $\pm 0.5^\circ$. In the no-shear experiments ($K = 0$), the cylinder experienced a small positive lift coefficient, that indicated a $\sim 1^\circ$ misalignment of the force balance with the approach flow. The C_D and C_L data in Figs. 7 and 8 and Table 2, and the pressure data presented in Fig. 9, were corrected for this bias error caused by the misalignment.

The total mean aerodynamic force, represented by the dimensionless total force coefficient, $C_T (= (C_L^2 + C_D^2)^{1/2})$, and its direction with respect to the mean flow, β (see Fig. 2), were also calculated; results are summarized in Table 2. In a low to moderate shear flow, the magnitude of the total mean aerodynamic force acting on the cylinder is lower than for the no-shear case, $K = 0$, where it consists only of the drag force. This result indicates that the reduction in the cylinder drag force in a shear flow is not caused solely by a rotation of the total (or resultant) aerodynamic force vector.

5.3. Pressure distribution and flow field

The mean static pressure distribution on the surface of the cylinder (Fig. 9) was also measured. From Fig. 9 it is seen that low to moderate shear increases the mean base pressure compared to the no-shear case, $K = 0$. This result is consistent with the observed reduction in the mean drag coefficient and a reduction in near-wake width (Griffin, 1981).

The mean pressure drag coefficient and the lift coefficient were found by integrating the $C_P(\theta)$ data. The results were similar to those obtained from direct measurement using the force balance, Table 2, with a reduction in the pressure drag coefficient at $K = 0.07$ compared to the no-shear case, $K = 0$, and a small mean lift force directed towards the low-velocity side. Because of the limited number of pressure measurements, and the need to rotate the cylinder, these force data have a higher measurement uncertainty than those measured directly with the force balance, as given in Table 2.

Closer examination of the surface static pressure distribution in a planar shear flow (see Fig. 9) shows that it has a small degree of asymmetry. On the high-velocity side, the points of minimum pressure and separation move further back on the surface of the cylinder, while on the low-velocity side, these points move further forward on the surface of the cylinder. In each case the shift is small, less than 5°, for $K = 0.07$; Hayashi et al. (1991) observed a much more pronounced shift at a higher shear parameter of $K = 0.15$. The rearward movement of the separation point on the high-velocity side is consistent with a narrowing of the near-wake region in the presence of the planar shear flow. This rotation or asymmetry of the mean static pressure distribution, indicated by the movement of the points of minimum pressure and separation, is also the origin of the steady mean lift force experienced by the circular cylinder in the shear flow (Hayashi et al., 1991).

Apart from the movement of these points in the shear flow, the stagnation point is seen to shift to the higher velocity side of the flow, although for $K = 0.07$ the shift is very small, approximately 1° (and close to the angular positioning uncertainty of the cylinder, which was estimated at $\pm 0.5^\circ$). This shift in the stagnation point is more pronounced under higher shear conditions, $+6^\circ$ for $K = 0.15$ as reported by Hayashi et al. (1991). Both the asymmetry in the $C_P(\theta)$ data and the shift in the stagnation point are consistent with the rotation of the resultant aerodynamic force vector, β, of approximately -3° for $K = 0.07$ (see Table 2).

Fig. 10 shows some wake velocity profiles for a circular cylinder in shear flow. At $x/D = 10$, the location of the minimum wake velocity is shifted to the low-velocity side by $-0.1D$. This small shift is consistent with the asymmetry in the surface static pressure distribution, the shift in the stagnation point to the high-velocity side, and the rotation of total aerodynamic force vector noticed under shear.

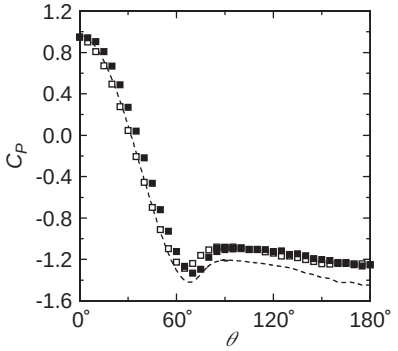

Fig. 9. Mean static pressure distribution on a circular cylinder in a uniform planar shear flow, $\mathrm{Re} = 7.0 \times 10^4$, $K = 0.07$: ■, high-velocity side; □, low-velocity side. -----, No shear case, $K = 0$. The experimental uncertainty in θ is estimated at $\pm 0.5^\circ$. The experimental uncertainty in C_P is estimated at ± 0.02.

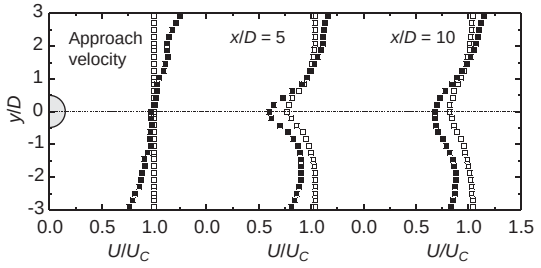

Fig. 10. Wake mean velocity profiles for a circular cylinder: ■, uniform planar shear flow, $K = 0.07$, $\mathrm{Re} = 7.0 \times 10^4$; □, uniform flow (no-shear case), $K = 0$, $\mathrm{Re} = 6.0 \times 10^4$. The experimental uncertainty in U/U_C is estimated at $\pm 1\%$.

6. Conclusions

An experimental investigation was undertaken of a single isolated circular cylinder immersed in a uniform planar shear flow in the subcritical Reynolds number regime, $\mathrm{Re} = 4.0 \times 10^4 - 9.0 \times 10^4$, and at low to moderate shear, $K = 0.02 - 0.07$. The study was motivated by a lack of extensive experimental data for the planar shear flow case, particularly in the subcritical regime, and some disagreements between the various experimental and numerical results reported in the literature. In particular, there are few if any reported measurements of the Strouhal number in the subcritical regime and for the mean lift coefficient.

It was found that within the subcritical regime, low to moderate shear did not appreciably influence the Strouhal number. Published data at higher shear parameters have indicated that the Strouhal number increases with K, and the present data do not necessarily contradict this finding. The previously published data were also at lower Reynolds numbers than the present study, however, so it remains to be seen whether this increase in Strouhal number is independent of the Reynolds number.

Low to moderate shear also has the effect of lowering the mean drag coefficient of the circular cylinder. This behaviour is consistent for a wide range of Reynolds numbers and the reduction in drag becomes more pronounced as the level of shear is increased. The circular cylinder in a planar shear flow also experiences a small steady mean lift force directed towards the low-velocity side, which increases in magnitude as the shear increases. Amounting to less than 5% of the drag force when $K = 0.07$, however, this lift force was very difficult to measure accurately owing to the angular positioning uncertainty of the force balance and cylinder.

The total mean aerodynamic force experienced by the cylinder is also lower in a planar shear flow, and therefore the reduction in the drag force, which is accompanied by an increase in the mean base pressure, cannot be attributed entirely to a simple rotation of the aerodynamic force vector. The lift force results from the asymmetric mean static pressure distribution on the surface of the cylinder. A small asymmetry is also evident in the wake mean velocity profile.

The increase in the Strouhal number, the increase in the mean base pressure coefficient, and the reduction in the mean drag coefficient, may be caused by a narrowing, or reduction in width, of the cylinder near wake in a planar shear flow. This narrowing of the near wake is supported by the asymmetric mean static pressure distribution, in which the points of minimum pressure and separation shift rearward on the high-velocity side.

Acknowledgements

The support of the Natural Sciences and Engineering Research Council (NSERC) of Canada and the University of Saskatchewan is gratefully acknowledged. The assistance of D. Braun, D. Deutscher, J.L. Heseltine, M.D. Richards, and Engineering Shops, is also appreciated.

References

Adachi, T., Kato, E., 1975. Study on the flow about a circular cylinder in shear flow. Journal of the Japan Society for Aeronautical and Space Sciences 23, 311–319 (in Japanese).

Ahmed, F., Lee, B.E., 1997. The production of shear flow profiles in a wind tunnel by a shaped honeycomb technique. ASME Journal of Fluids Engineering 119, 713–715.

Akosile, O.O., 2002. Circular cylinders in a uniform planar shear flow. M.Sc. Thesis, Department of Mechanical Engineering,. University of Saskatchewan, Canada.

Akosile, O.O., Sumner, D., 2001. Design of a shear flow generator for wind tunnel testing of circular cylinders. In: Swamidas, A., et al. (Ed.), Proceedings of the 18th Canadian Congress of Applied Mechanics. St. John's, Canada, pp. 363–364.

Ayukawa, K., Ochi, J., Kawahara, G., Hirao, T., 1993. Effects of shear rate on the flow around a square cylinder in a uniform shear flow. Journal of Wind Engineering and Industrial Aerodynamics 50, 97–106.

Bearman, P.W., Zdravkovich, M.M., 1978. Flow around a circular cylinder near a plane boundary. Journal of Fluid Mechanics 89, 33–47.

Castro, I.P., 1976. Some problems concerning the production of a linear shear flow using curved wire-gauze screens. Journal of Fluid Mechanics 76, 689–709.

Griffin, O.M., 1981. Universal similarity in the wakes of stationary and vibrating bluff structures. ASME Journal of Fluids Engineering 103, 52–58.

Griffin, O.M., 1985. Vortex shedding from bluff bodies in a shear flow: a review. ASME Journal of Fluids Engineering 107, 298–306.

Hayashi, T., Yoshino, F., Waka, R., 1991. An analytical evaluation of the aerodynamic forces acting on a circular cylinder in a uniform shear flow. In: Morris, M.J., et al. (Ed.), Proceedings of the First ASME/JSME Fluids Engineering Conference, FED-Vol. 112. Portland, OR, pp. 83–88.

Hayashi, T., Yoshino, F., Waka, R., 1993. The aerodynamic characteristics of a circular cylinder with tangential blowing in uniform shear flows. JSME International Journal Series B 36, 101–112.

Hwang, R.R., Sue, Y.C., 1997. Numerical simulation of shear effect on vortex shedding behind a square cylinder. International Journal for Numerical Methods in Fluids 25, 1409–1420.

Jordan, S.K., Fromm, J.E., 1972. Laminar flow past a circle in shear flow. Physics of Fluids 15, 972–976.

Karnik, U., Tavoularis, S., 1987. Generation and manipulation of uniform shear with the use of screens. Experiments in Fluids 5, 247–254.

Kiya, M., Arie, M., Tamura, H., 1979. Forces acting on circular cylinders placed in a turbulent plane mixing layer. Journal of Industrial Aerodynamics 5, 13–33.

Kiya, M., Tamura, H., Arie, M., 1980. Vortex shedding from a circular cylinder in moderate-Reynolds-number shear flow. Journal of Fluid Mechanics 141, 721–735.

Kotansky, D.R., 1966. The use of honeycomb for shear flow generation. AIAA Journal 4, 1490–1491.

Kwon, T.S., Sung, H.J., Hyun, J.M., 1992. Experimental investigation of uniform-shear flow past a circular cylinder. ASME Journal of Fluids Engineering 114, 457–460.

Lei, C., Cheng, L., Kavanagh, K., 2000. A finite difference solution of the shear flow over a circular cylinder. Ocean Engineering 27, 271–290.

Owen, P.R., Zienkiewicz, H.K., 1957. The production of uniform shear flow in a wind tunnel. Journal of Fluid Mechanics 2, 521–531.

Phillips, J.C., Thomas, N.H., Perkins, R.J., Miller, P.C.H., 1999. Wind tunnel velocity profiles generated by differentially spaced flat plates. Journal of Wind Engineering and Industrial Aerodynamics 80, 253–262.

Saha, A.K., Biswas, G., Muralidhar, K., 1999. Influence of inlet shear on structure of wake behind a square cylinder. Journal of Engineering Mechanics 359–363.

Saha, A.K., Biswas, G., Muralidhar, K., 2001. Two-dimensional study of the turbulent wake behind a square cylinder subject to uniform shear. ASME Journal of Fluids Engineering 123, 595–603.

Sumner, D., Wong, S.S.T., Price, S.J., Païdoussis, M.P., 1999. Fluid behaviour of side-by-side circular cylinders in steady cross-flow. Journal of Fluids and Structures 13, 309–338.

Sung, H.J., Chun, C.K., Hyun, J.M., 1995. Experimental study of uniform shear past a rotating cylinder. ASME Journal of Fluids Engineering 117, 62–67.

Szepessy, S., 1993. On the control of circular cylinder flow by end plates. European Journal of Mechanics B/Fluids 12, 217–244.

Tamura, H., Kiya, M., Arie, M., 1980. Numerical study on viscous shear flow past a circular cylinder. Bulletin of the JSME 23, 1952–1958.

Wu, T., Chen, C.-F., 2000. Laminar boundary-layer separation over a circular cylinder in uniform shear flow. Acta Mechanica 144, 71–82.

Yoshino, F., Hayashi, T., 1984. Numerical solution of flow around a rotating circular cylinder in uniform shear flow. Bulletin of the JSME 27, 1850–1857.

Zdravkovich, M.M., 1977. Review of flow interference between two circular cylinders in various arrangements. ASME Journal of Fluids Engineering 99, 618–633.

Zdravkovich, M.M., 1997. Flow Around Circular Cylinders, Vol. 1, Oxford University Press, Oxford.